Exploring the Thin Talangakar Formation Sandstone Using Integrated Seismic Multi-Attribute Analysis and Spectral Decomposition in Kuang Area, South Sumatra Basin*

Noor Cahyo Wibowo[1]

Search and Discovery Article #10900 (2016)
Posted December 26, 2016

*Adapted from traditional manuscript, with poster presented at AAPG/SEG International Conference & Exhibition, Cancun, Mexico, September 6-9, 2016

[1]Geophysics, Colorado School of Mines, Golden, CO (noorcahyo@gmail.com)

Abstract

The Kuang area, which is located in a marginal area of the South Sumatra Basin, contains relatively thin Talangakar Formation sediments compared to the overall thickness in the basin. This thin section indicates that the condition of the area during Talangakar Formation deposition was a stable pre-Tertiary basement high. Of seven exploration wells within the study area, only one well has a hydrocarbon accumulation in the Talangakar Formation sandstone. The main issue with exploration targeting Talangakar Formation sandstone in the study area is the sandstone reservoir distribution. This study describes the distribution of sandstone members within the Oligocene-Miocene Talangakar Formation and their depositional environment system.

A multi-attribute seismic analysis was conducted to build a pseudo-gamma-ray cube for delineation of the distribution of Talangakar Formation sandstone within recently acquired 355 km^2 of 3D seismic data. Multi-attribute seismic training using a step-wise algorithm reveals the best correlation combination of transform using four operators and five attributes. To overcome the issue of thin reservoir thickness, spectral decomposition was conducted as an additional static analysis to resolve the details of sandstone distribution. The resulting spectral decomposition maps at 25 Hz confirm the sandstone distribution trend of the predicted gamma-ray maps. Both spectral decomposition and predicted gamma-ray maps show that most of the exploration wells penetrated poor sandstone reservoir.

The geological interpretation was undertaken through an integrated analysis of paleogeography, well data, -gamma ray and spectral decomposition maps. The major sedimentation direction of the Talangakar Formation in the area is to the southwest, with transgression phase to the northeast. The depositional environment of the lower member is interpreted as a fluvio-deltaic system along a NE-SW direction with a channel pattern in the eastern part. The upper member has a NW-SE sandstone pattern deposited in a shallow-marine depositional system. The study result answers the failure of most exploration wells and describes the potential of the Talangakar Formation sandstone in the area. Some new prospects can be identified from a combination of well developed sandstone areas and structural-stratigraphic traps.

Introduction

The South Sumatra Basin is a back-arc basin system located in the southern part of Sumatra Island in Indonesia. The basin is a prolific hydrocarbon producer with estimated ultimate recoverable reserves around 3 billion barrels of oil and 22 TCF of gas (Ginger and Fielding, 2005). The major reservoirs in the basin are Baturaja Formation carbonate, Talangakar Formation sandstone and Pre-Tertiary basement. Reserves from the Talangakar sandstone accounts for 46% of the total reserves in the basin. The study area lies on the Kuang high area at the southern part of the basin (Figures 1 and 2). Structurally, the area is a local high south of the basin depocenter. The main reservoir rocks in the study area are lower Miocene carbonates of the Baturaja Formation (BRF) and upper Oligocene to lower Miocene clastics of the Talangakar Formation (TAF).

Recent studies of the distribution of TAF sandstone covering the study area have been undertaken by numerous authors. However, those studies have never been made in detail due to limited data availability. Tamtomo et al. (1997) has described the Talangakar sandstone distribution model based on formation thickness from well data. He found that TAF was deposited in the Kuang area with marginal thicknesses due to local basement configuration. A more recent study was undertaken by Ginger and Fielding (2005) with a geological interpretation of the depositional environment on a regional basin-wide scale.

The study area has a mature petroleum system surrounded by abundant oil and gas fields. There is one oil field and several discovered structures in the area that have not been developed due to the limitation of identified reserves. Recently a rise in gas prices and the availability of a nearby gas facility have stimulated the development of suspended discovered structures. In order to support the field development and further exploration campaign, 3D seismic data were recently acquired. This article describes the delineation of the sandstone reservoir of Talangakar in the area, using 3D seismic and available well log data.

According to well data used in the study, the sandstone thicknesses range from less than 1 m to 4 m. Due to the thickness of Talangakar sandstone, direct seismic attributes have failed to provide an accurate model. Seismic multi-attribute analysis was selected to investigate pseudo-properties of interest. To overcome the formation thickness issue, static analysis of spectral decomposition was conducted. In this case, spectral decomposition is used to check the accuracy of the multi-attribute analysis results. The geological interpretation was based on an integrated analysis of well data, paleogeography, pseudo-gamma ray and spectral decomposition maps. The study results provide a useful input of reservoir distribution for an integrated field development plan and further exploration play of TAF in the Kuang area.

Talangakar Formation Sandstone

The Talangakar Formation (TAF) was identified as fill sediments in a late-stage graben and early post-rift stage, deposited during the late Oligocene to early Miocene. During transgressive phases sediments consist of fluvial and deltaic sediments that grade basinward into marginal marine sediments (Figures 3 and 4). Lithologically, the TAF consists of interbedded sandstones, marine shales, mudstones, siltstones, and coals. There are two members of TAF, namely the great sand member (GRM), or Lower TAF (LTAF), and transition member (TRM), or Upper TAF (UTAF). Tamtomo et al. (1997) and Ginger and Fielding (2005) identified the depositional environment of Lower TAF in the Kuang and surrounding area as a fluvial to deltaic system, whereas the Upper TAF was deposited in a shallow marine environment.

The Kuang area, which is located in the southern marginal area of the basin, contains relatively thin TAF sediments compared to the overall TAF thickness in the basin. This thin unit indicates that the setting of the area during TAF deposition was a stable pre-Tertiary basement high. The gross thickness of the TAF section penetrated by the available wells varies slightly across the Kuang area, reflecting the variability in the accommodation space. According to the well data, only, TRM, or UTAF, developed in the study area with thickness range from 15 to 77 m, whereas sandstone thickness is less than 1 m to 4 m. The tops of the TAF were penetrated at around 1568-2005 m below the earth's surface.

Most of exploration discoveries (wells S, M, D, R, B and U) found hydrocarbons in the BRF carbonate reservoir (Figure 5). However, only the U structure has a hydrocarbon accumulation in the TAF sandstone reservoir. The main issue with exploration targeting TAF in the Kuang area is the sandstone reservoir distribution. Structure U in the eastern area has relatively good sandstone quality, whereas the other six exploration wells penetrated an area of structures that has poor to moderate sandstone reservoir quality. Productive reservoir layers within the U structure consist of lower and upper members of UTAF.

Well correlations (Figures 6 and 7) show the distribution of UTAF members in detail. The upper member is well developed over all the study area, whereas the lower member is absent in some parts of the northwest area (wells S and D). The TAF overlies the syn-rift sediments of the Lahat Formation (LAF), and some of them directly overlie the pre-Tertiary basement where the LAF is absent. A time thickness map (isochron) of the TAF from seismic interpretation shows a thickness trend of NE-SW (Figure 8). The southeast area appears to have thin sediments, as does the northwest part. Seismically, two UTAF members cannot directly be interpreted in the seismic section due to vertical resolution (Figure 9). Multi-attribute seismic analysis was conducted for further identification of UTAF members and their sandstone lateral distribution.

Seismic Multi-attribute Analysis

Seismic multi-attribute analysis has been recently used as a reservoir characterization tool to delineate the distribution of reservoir properties. Multi-attribute analysis is a broad term for using multiple seismic attributes to predict log properties through a geostatistical correlation. The method was initially introduced by Schultz et al. (1994). The multi-attribute analysis in this study is a multivariate geostatistical technique, as introduced by Hampson et al. (2001). The processes involved in this methodology include calibration of well log and seismic data, multi-attribute training and population of predicted log into the seismic volume.

The main objective of multi-attribute training is to find the best combination of operator length and attributes in predicting a property of interest. The reliability of the resulting combination is estimated by cross-correlating the predicted log with the actual log. Multi-attribute analysis in this study used a stepwise regression algorithm and a linear transform of weighted attributes. Those attributes can be either linear or nonlinear. The way the algorithm works has been described by Hampson et al. (2001):

1. Search for the best attribute that has the lowest prediction error.
2. Find the second attribute that if it is paired with the first attribute has the lowest prediction error.
3. Find the third attribute to build a triplet with the first and second selected attributes above, in which case the triplet has the lowest prediction error.
4. Continue the process as necessary.

This study uses 350 km^2 of post-stack 3D seismic and five well logs as input for the multi-attribute analysis process. The seismic data have a sampling interval of 2 milliseconds, with a minimum phase and reverse polarity in SEG standard. In order to trace the distribution of the TAF sandstone, this study targeted gamma ray as the property of interest. The actual gamma ray logs from wells S, D, R, L and U were used in the analysis. The multi-attribute training result revealed that the combination of 5 attributes and 4 operators produces the lowest average error to predict gamma ray (Figure 10). The 5 attributes are presented in Figure 11. A cross-plot of predicted and actual gamma ray in all five training wells has a correlation coefficient of 0.71 with an error margin of 34.8 gAPI (Figure 12). The resulting multi-attribute training was then populated within a 3D seismic volume to define a pseudo-gamma ray cube. The predicted gamma ray map for the upper member was extracted from the cube using the root mean square (RMS) of a 20 ms window.

Spectral Decomposition

Spectral decomposition provides a tool for imaging and mapping geological discontinuities and bed thickness within the seismic data (Partyka et al., 1999). The basic concept of spectral decomposition is to transform the seismic data from a typical time domain into a frequency domain. Displaying seismic data in the frequency domain might reveals the thin bed reflections that cannot be displayed in the time domain due to the resolution. Amplitude spectra at higher frequency slices correspond to thinner beds, whereas lower frequency slices correspond to thicker beds (Chopra and Mafurt, 2007). Spectral decomposition helps the interpreter quickly identify and define subsurface geological features.

Spectral decomposition analysis over a 3D seismic survey was undertaken to perform a qualitative analysis of the TAF sandstone delineation. The result was used to confirm the pseudo-gamma ray model produced by quantitative multi-attribute analysis. This study used two spectral decomposition algorithms, namely, Maximum Entropy Method (MEM) and Discrete Fourier Transform (DFT). Given that each TAF member has a thickness analysis window of less than 30 ms, the DFT algorithm does not display optimum spectral imaging. The resulting spectral decomposition map using the MEM algorithm was chosen because it has better static resolution than the result from the DFT algorithm.

Frequency slices were generated using the same 20 ms window as the multi-attribute analysis for the upper member. The amplitude map at 25 Hz frequency (Figures 13 and 14) confirm the pseudo-gamma ray map of the lower and upper members. The peak amplitude trend at the frequency slice shows an appropriate trend with low gamma ray distribution patterns. This static analysis demonstrates a good ability of seismic multi-attribute analysis to predict the gamma ray log.

Results and Discussion

Because the resulting maps of spectral decomposition and multi-attribute analysis have similar patterns, the interpretation utilizes only the RMS maps of the pseudo-gamma ray (Figures 15 and 16). The RMS gamma ray values on the map reflect the presence of sandstone within the map location. A low gamma ray value (0-50 gAPI, yellow to green colors) indicates a high net-to-gross ratio sandstone within the TAF. A middle gamma ray value (51-100 gAPI, orange to brown colors) represents a moderate to low net-to-gross ratio. A high gamma ray value (101-200 gAPI, blue to purple colors) means low sandstone content or even no sandstone present in the formation.

The pseudo-gamma ray map of the lower member shows low gamma ray values in the eastern part of the study area, including well U. This map is in accordance with the presence of a good sandstone reservoir within well U. The low gamma ray values exhibit a sinusoidal pattern considered indicative of a SW-NE channel. The TAF thickness map and regional geology of the study area suggest that the main direction of sediment transport is to the southwest. In contrast, the main transgression direction is to the northeast. The dip log of well R shows that sandstone was deposited in a channel (within the lower member) with a paleocurrent direction of S10W (Figure 17). The Formation Micro Imager (FMI) log of well B shows 0.2 m-thick sandstone deposited within a channel trending S75E (Figure 18). Those thin sandstones coincide with the gamma ray map of well B and R that has low net-to-gross ratio (Figure 15).

The sandstone of upper member has a NW-SE trend according to the low gamma ray values in the map (Figure 16). This trend is in agreement with the major regional transgressive direction to the northeast and major sedimentation direction to the southwest area with provenance from the northeast. This shallow-marine sandstone distribution implies possible paleo-shoreline trending NW-SE.

Previous exploration wells mostly targeted BRF carbonate and TAF sandstone simultaneously. In this case, carbonate reefs developed on local highs. This model answers why most of the exploration wells failed to find good TAF sandstone in the study area. Furthermore, the presence of high net-to-gross TAF sandstone is desired to have a good reservoir quality. On the other hand, the TAF sandstone reservoir needs enough shale as intraformational caprock to prevent the hydrocarbon from escaping to the BRF carbonate above it. To achieve a good trapping mechanism for hydrocarbon accumulation, further integrated evaluations of the petroleum system elements have to be investigated thoroughly. Potential stratigraphic and structural traps for Lower TAF are shown in Figure 19 and those traps for Upper TAF are shown in Figure 20.

This study provided a model of TAF sandstone reservoir distribution within the study area as one of five petroleum system elements. Overall, the potential of the lower member in the western part is low, whereas the east area has medium to high reservoir potential within the channels. Better potential of the upper member exists in a NW-SE direction across the study area.

Conclusion

The sandstone of the lower member is well developed in the eastern part of the study area within a fluvial-deltaic channel system. The channel has a major sedimentation direction to the southwest, grading to transitional sediment in the west. The sandstone of upper member is interpreted as shallow-marine sediment, with a NW-SE distribution trend across the study area. This study highlights a robust method of integrating seismic multi-attribute analysis and spectral decomposition to map the sandstone distribution of the subtle TAF. The study results can be applied in future exploration campaigns of the TAF to target possible good sandstone development in conjunction with further evaluations of other petroleum system elements.

Acknowledgments

The Author would like to thank to the following company and people for their contribution:
PERTAMINA for providing 3D seismic data set, well logs and software.
Dr. Djuhaeni and Dr. Prihadi Soemintadiredja for their invaluable advice, discussion and guidance during the study.

Dr. Thomas Davis, Dr. Robert Benson, Dr. Terence Young, Dr. Stephen Sonnenberg, and Dr. Azra Tutuncu for fruitful comments, supports and reviews for the paper writing.

Selected References

Chopra, S., and K. J. Marfurt, 2007, Seismic Attributes for Prospect Identification and Reservoir Characterization: Society of Exploration Geophysicists, Tulsa, OK, p. 130 (of 450p).

De Coster, G.L., 1974, The geology of the Central and South Sumatra: Proceedings Indonesian Petroleum Association 3rd Annual Convention, Jakarta, Indonesia, p. 77-110.

Ginger, D., and K. Fielding, 2005, The petroleum systems and future potential of the South Sumatra Basin: Proceedings Indonesian Petroleum Association 30th Annual Convention, Jakarta, Indonesia, p. 67-89.

Hampson, D., J.S. Schuelke, and J.A. Quirein, 2001, Use of multi-attribute transforms to predict log properties from seismic data: Geophysics, v. 66, p. 220-236.

Partyka, G., J. Gridley, and J. Lopez, 1999, Interpretational applications of spectral decomposition in reservoir characterization: The Leading Edge, v.18, p. 353-360.

Schultz, P. S., S. Ronen, M. Hattori, and C. Corbett, 1994, Seismic-guided estimation of log properties, Part 1: A data-driven interpretation methodology: The Leading Edge, v.13/5, p. 305-311.

Tamtomo, B., I. Yuswar, and E. Widianto, 1997, Transgressive Talang Akar sands of the Kuang area, south Sumatra basin: Origin, distribution and implication for exploration play concept: Proceedings of the Petroleum Systems of SE Asia and Australasia Conference, Indonesian Petroleum Association, Jakarta, Indonesia, p. 699-708.

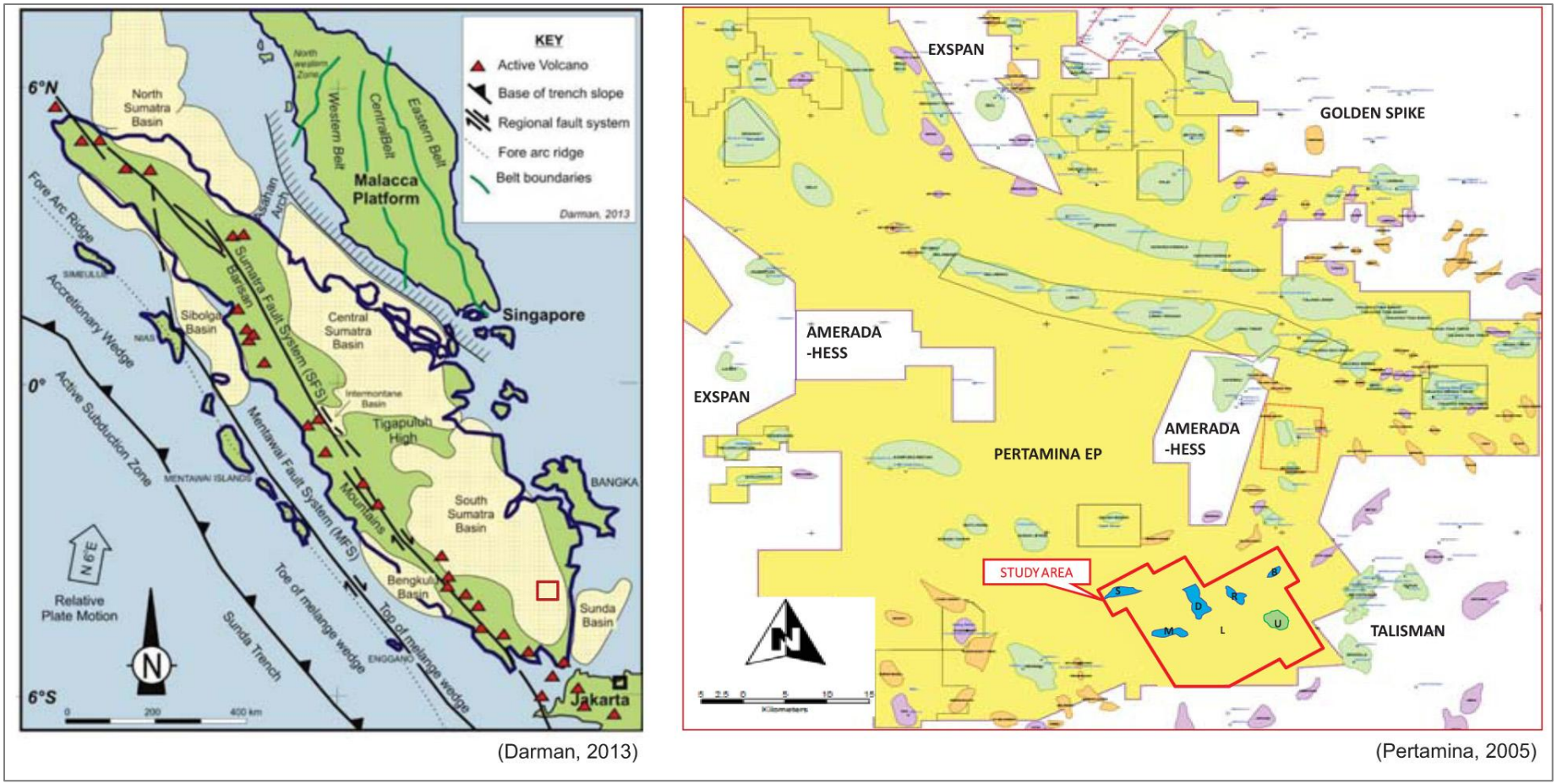

Figure 1. Location maps of study area in the southern part of the South Sumatra Basin, Indonesia.

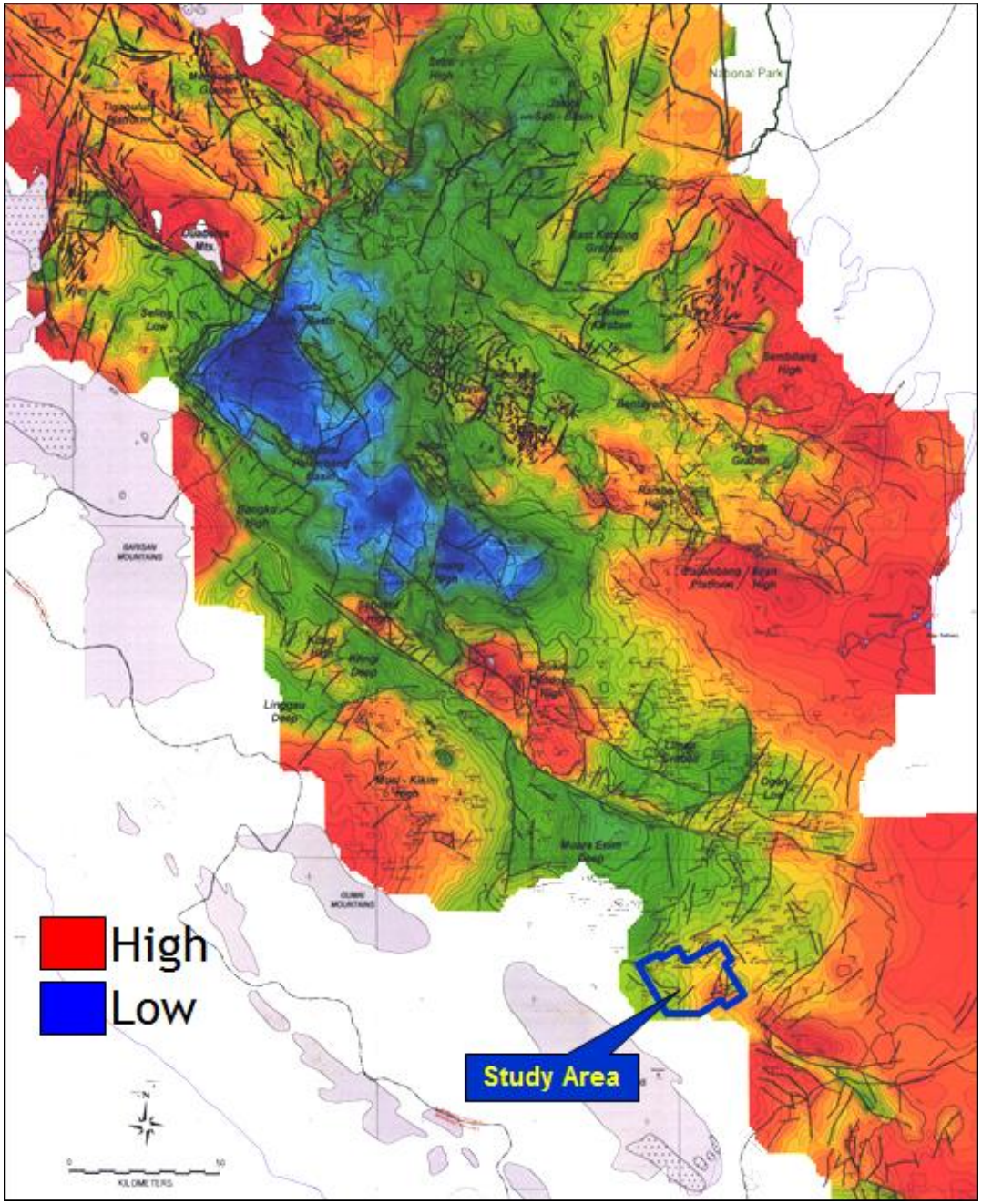

Figure 2. Structural map: the study area structurally is a local high to the southeast of the basin depocenter.

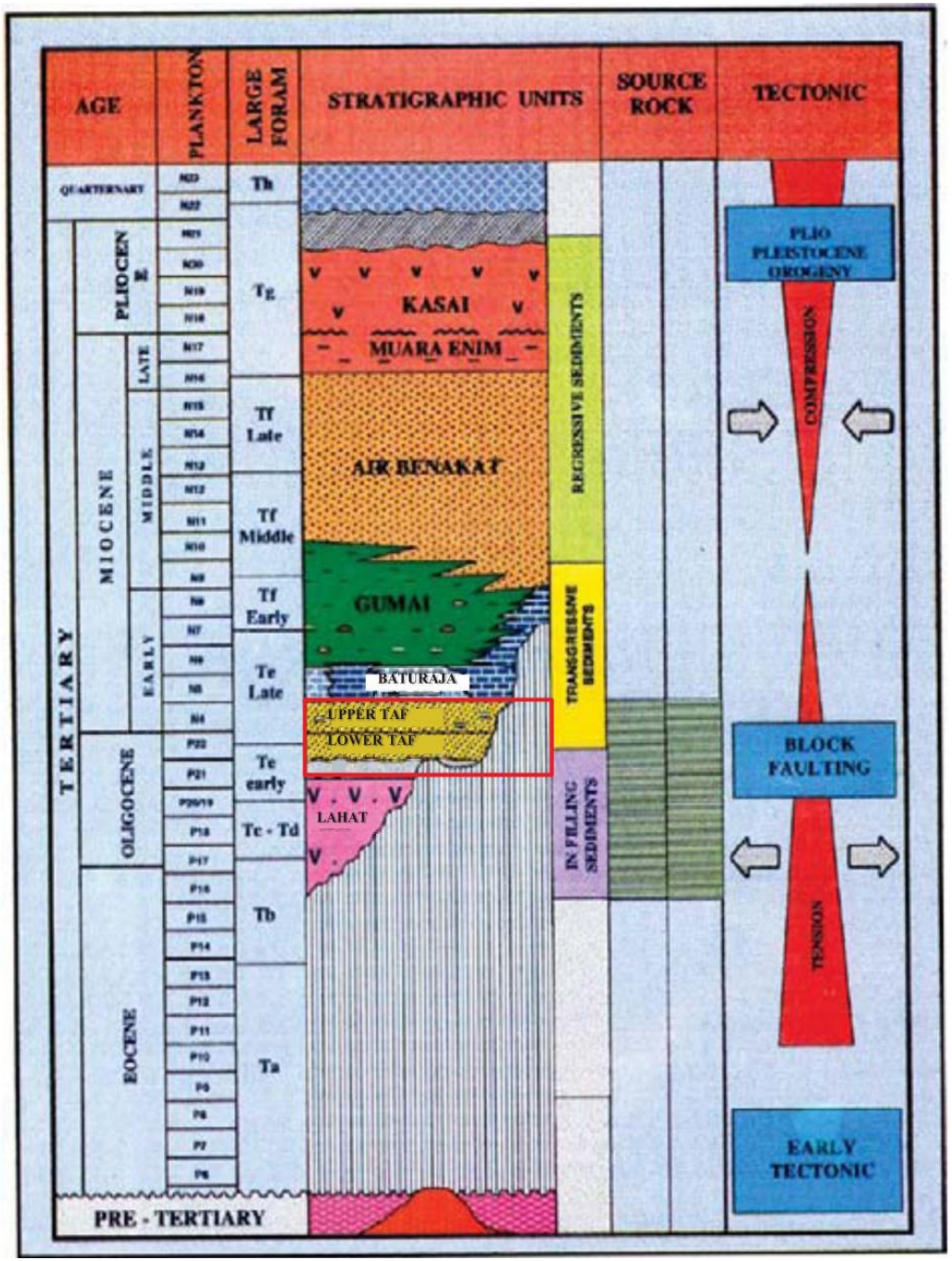

Figure 3. Stratigraphy of the South Sumatra Basin, including zonation foraminifera, source rocks, and related tectonic events (from Tamtomo et al., 1997).

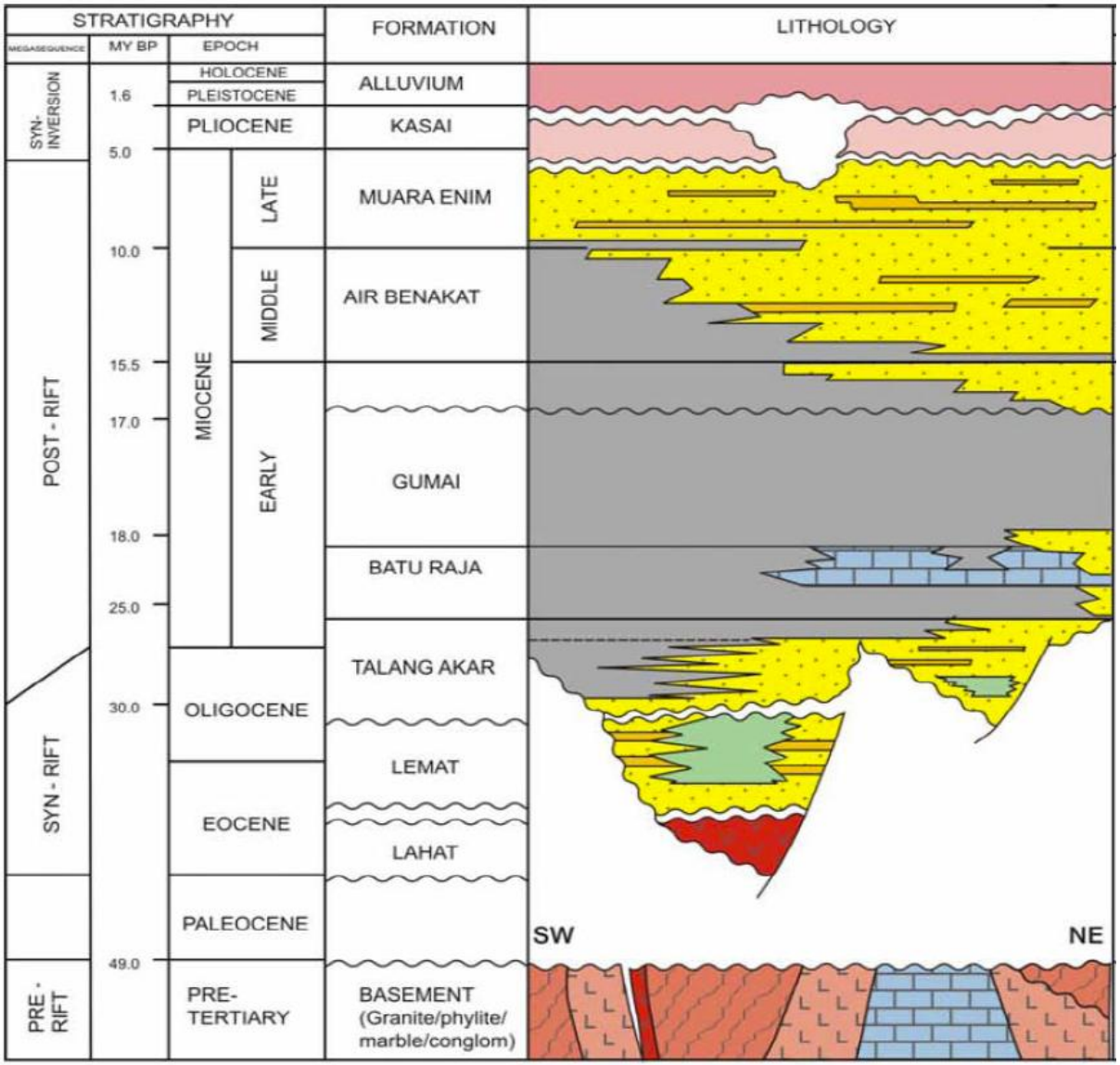

Figure 4. Simplified stratigraphic column of the South Sumatra Basin (Ginger et al., 2005). The study area lies in the southeast area of the basin, with an exploration objective of upper Oligocene to lower Miocene Talangakar Formation (red rectangle).

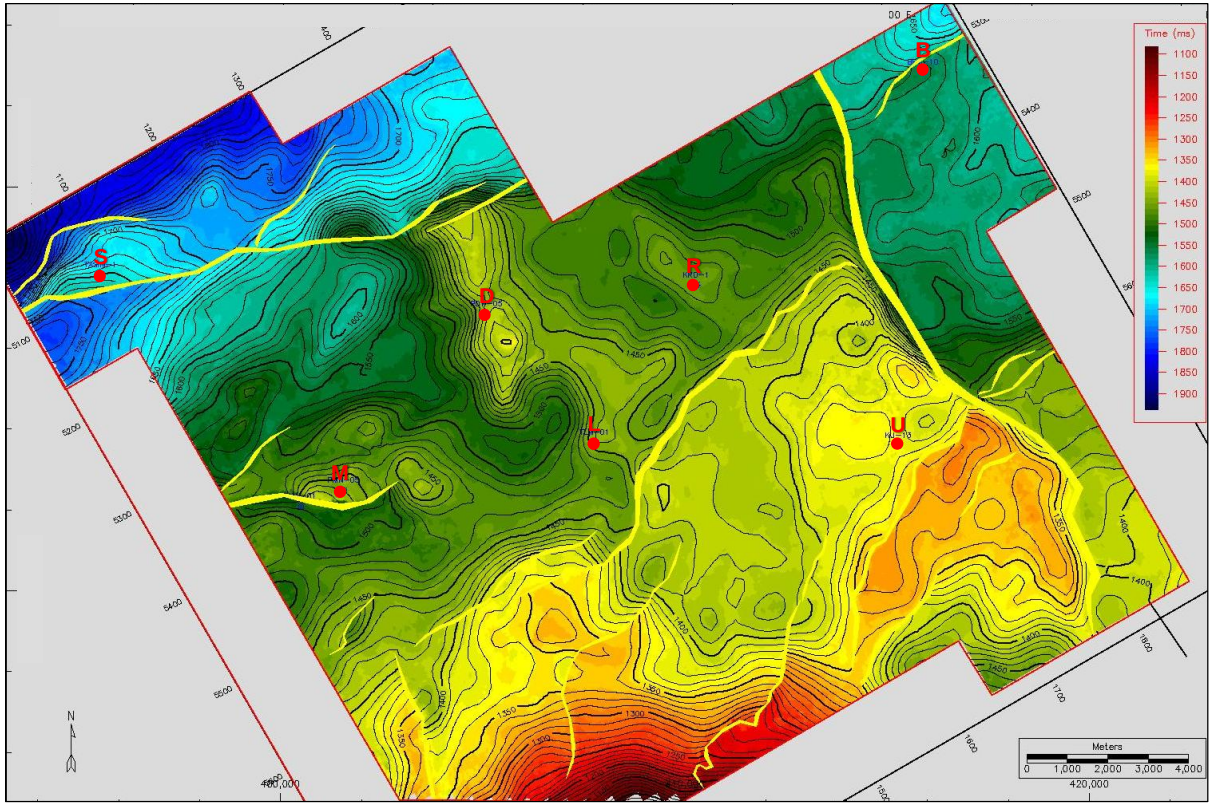

Figure 5. The time structure map of the Talangakar Formation top. The study utilized 355 km^2 of 3D seismic and data from 7 wells. One of those wells is located in an existing oil field (U); five wells are located in suspended structures (S, M, D, B and R); and the last well (L) is dry.

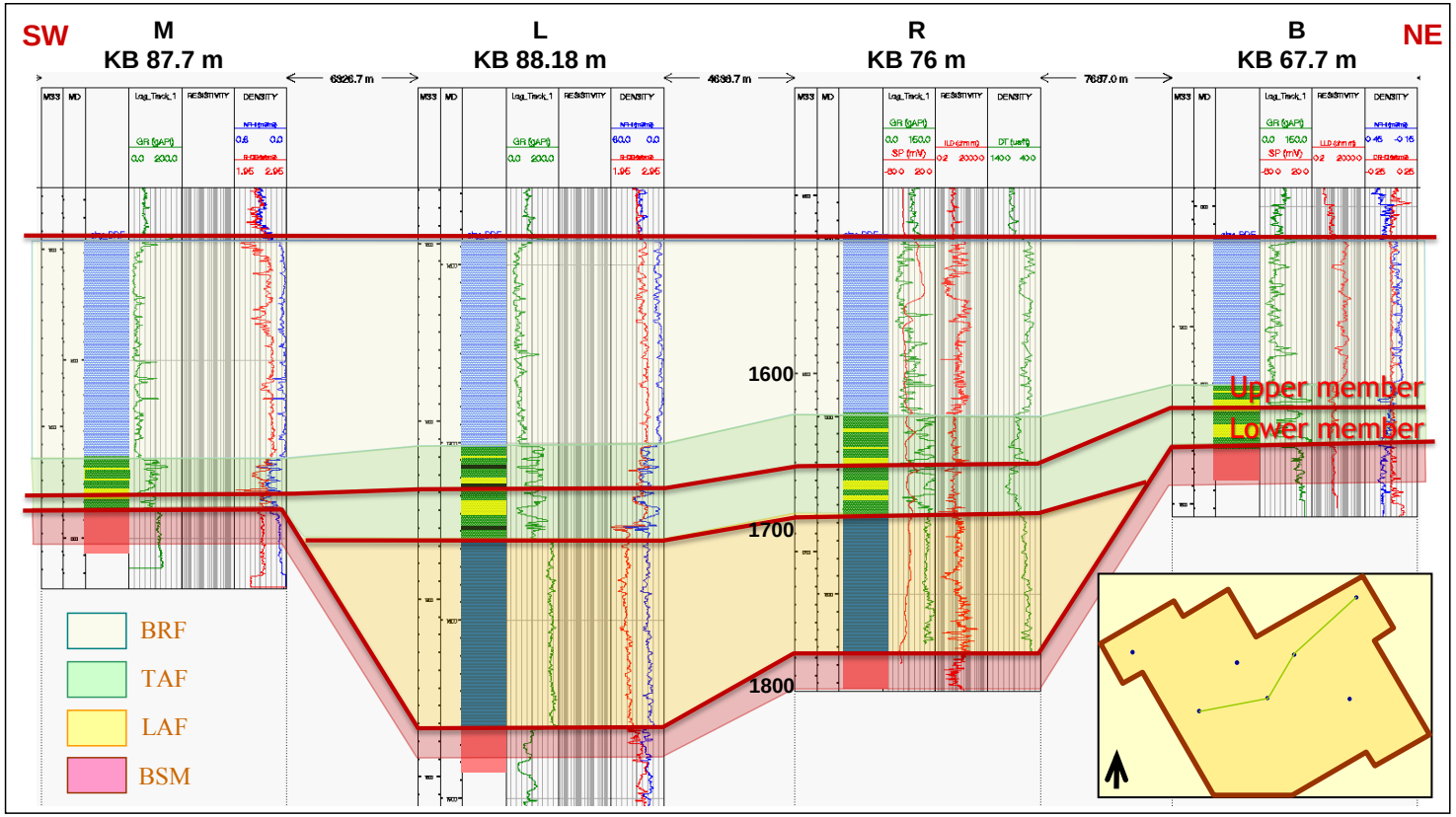

Figure 6. NE-SW structural correlation of the Talangakar Formation (TAF). Both the upper member and lower member are encountered in wells M, L, R and B.

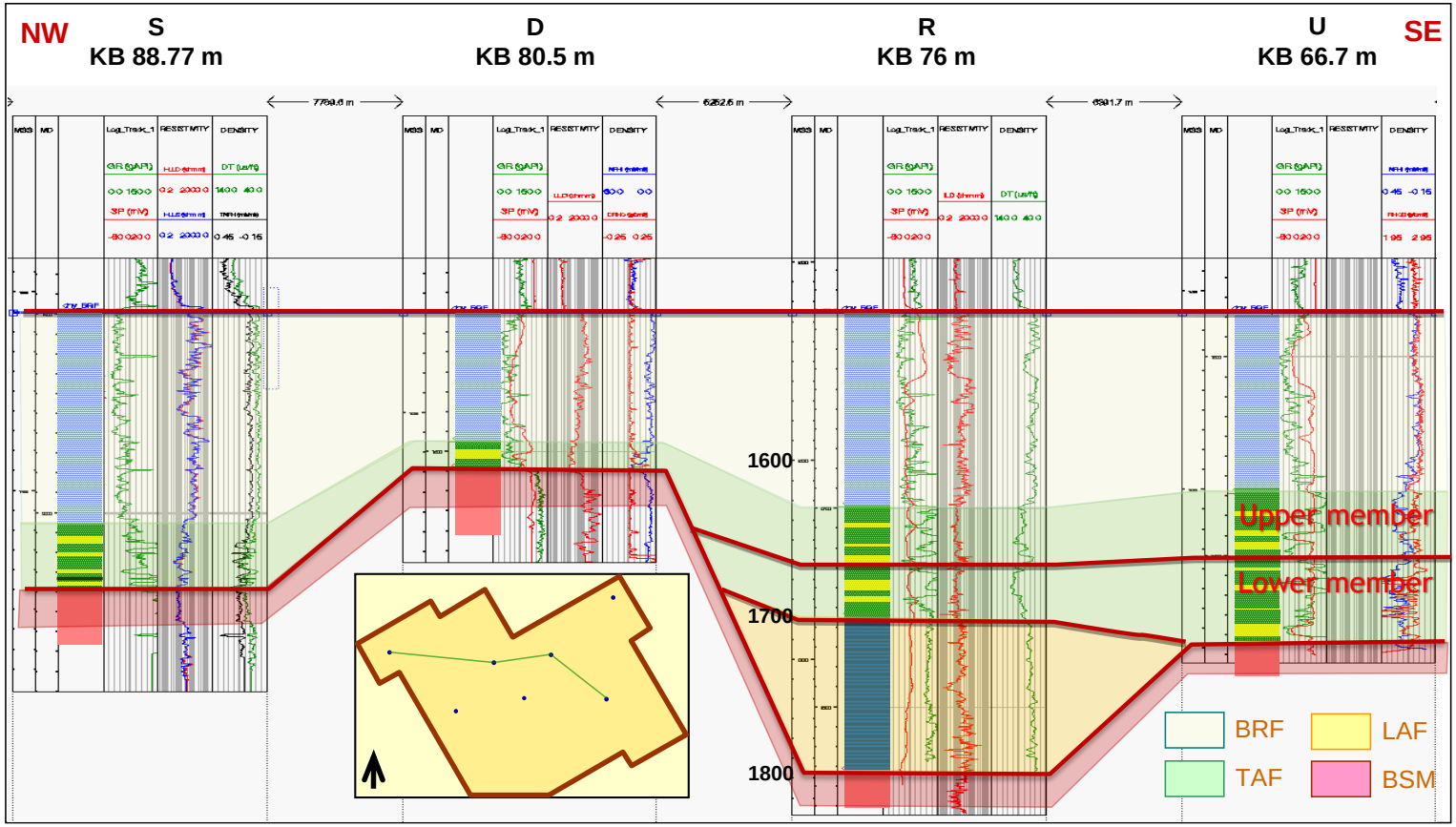

Figure 7. NW-SE structural correlation of the Talangakar Formation (TAF). The upper member is encountered in wells S, D, R and U, whereas the lower member is absent in wells S and D.

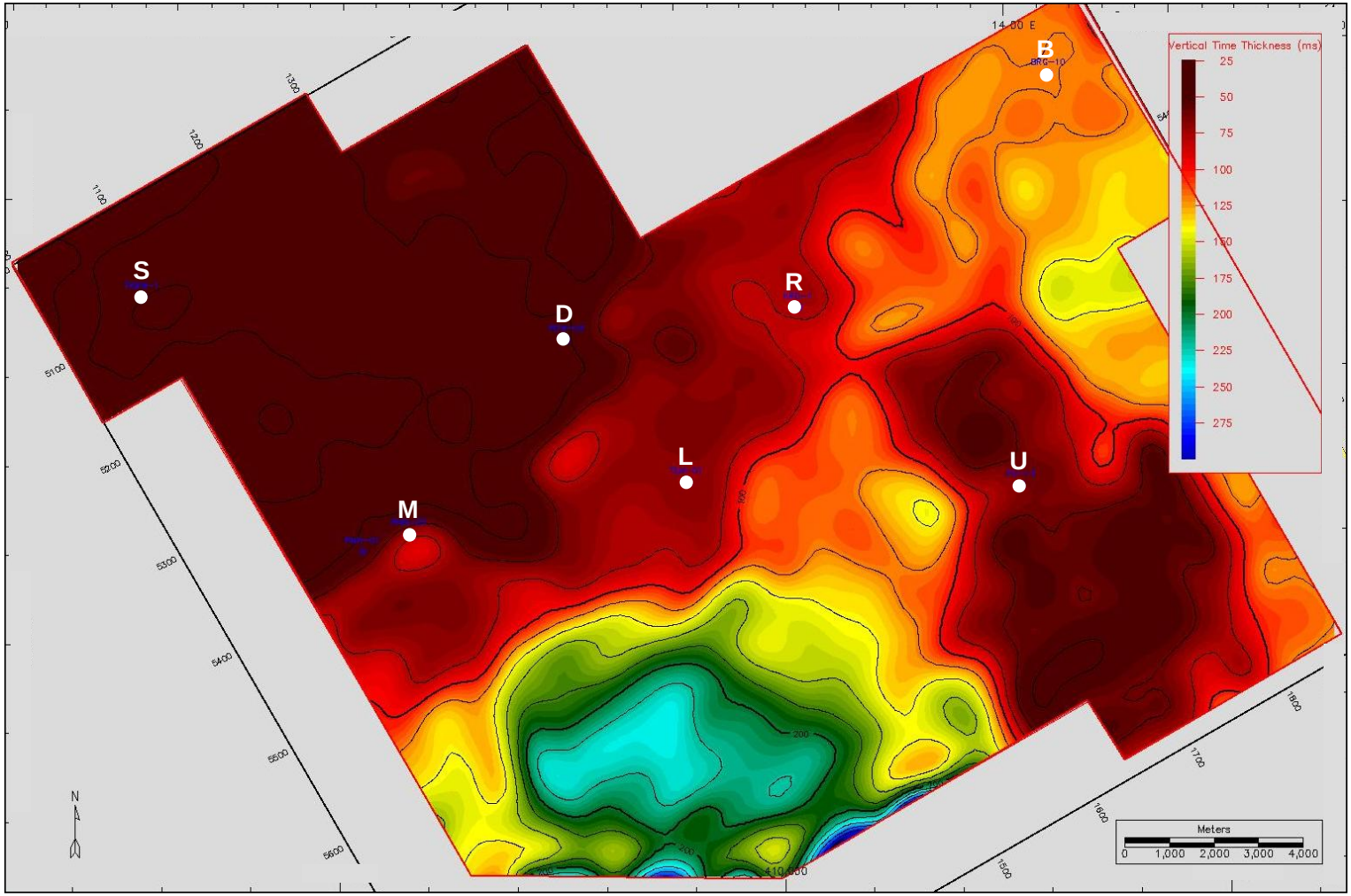

Figure 8. Time thickness map of the Talangakar Formation (TAF). According to the regional setting, the major sedimentation direction of the TAF in the study area is to the southwest, with provenance from a local high in the northeastern area.

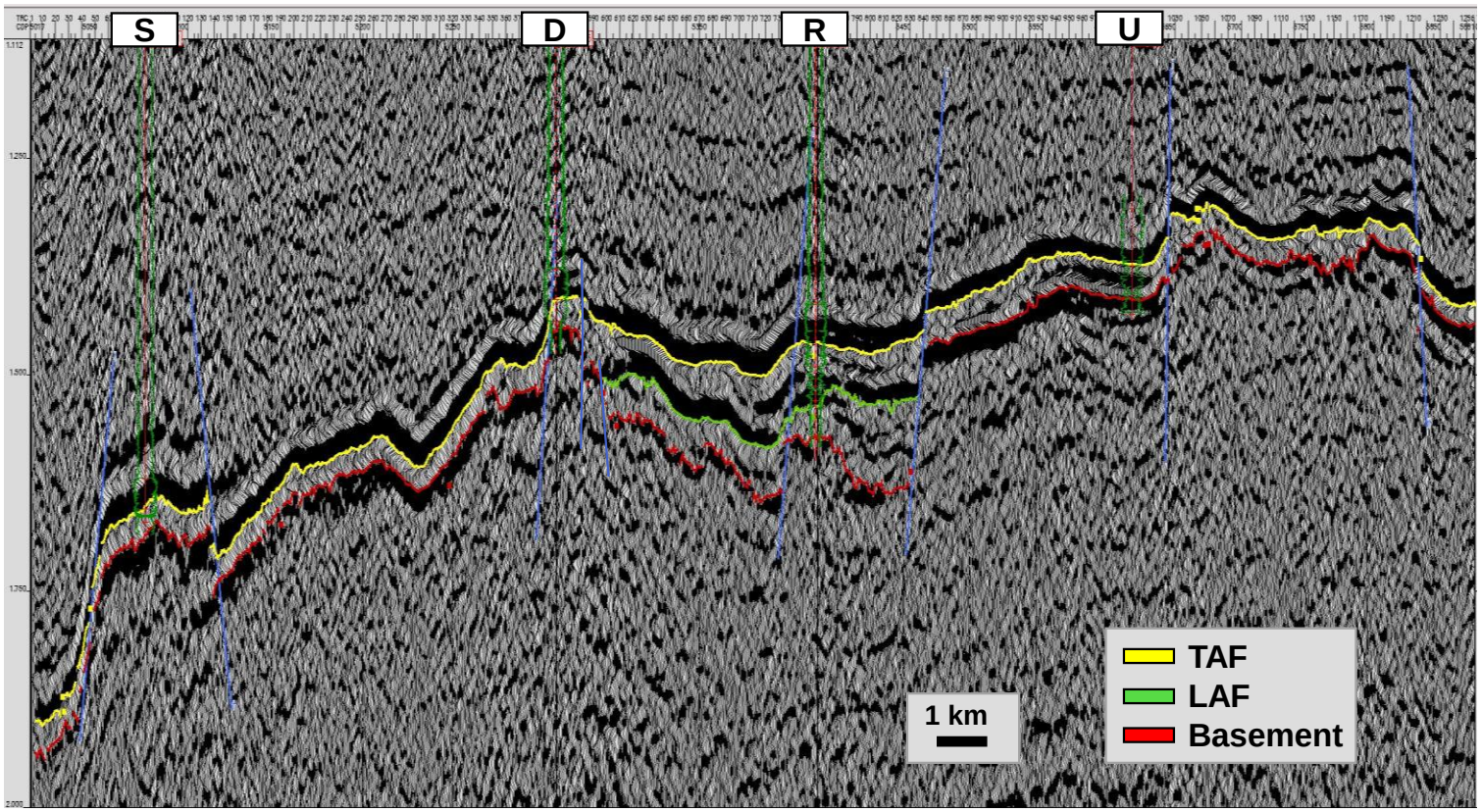

Figure 9. NW-SE seismic section across wells S, D, R, and U shows a relatively thin Talangakar Formation (TAF). In part of the area, the top of the lower member cannot be interpreted directly on the seismic section due to the limitation of seismic resolution.

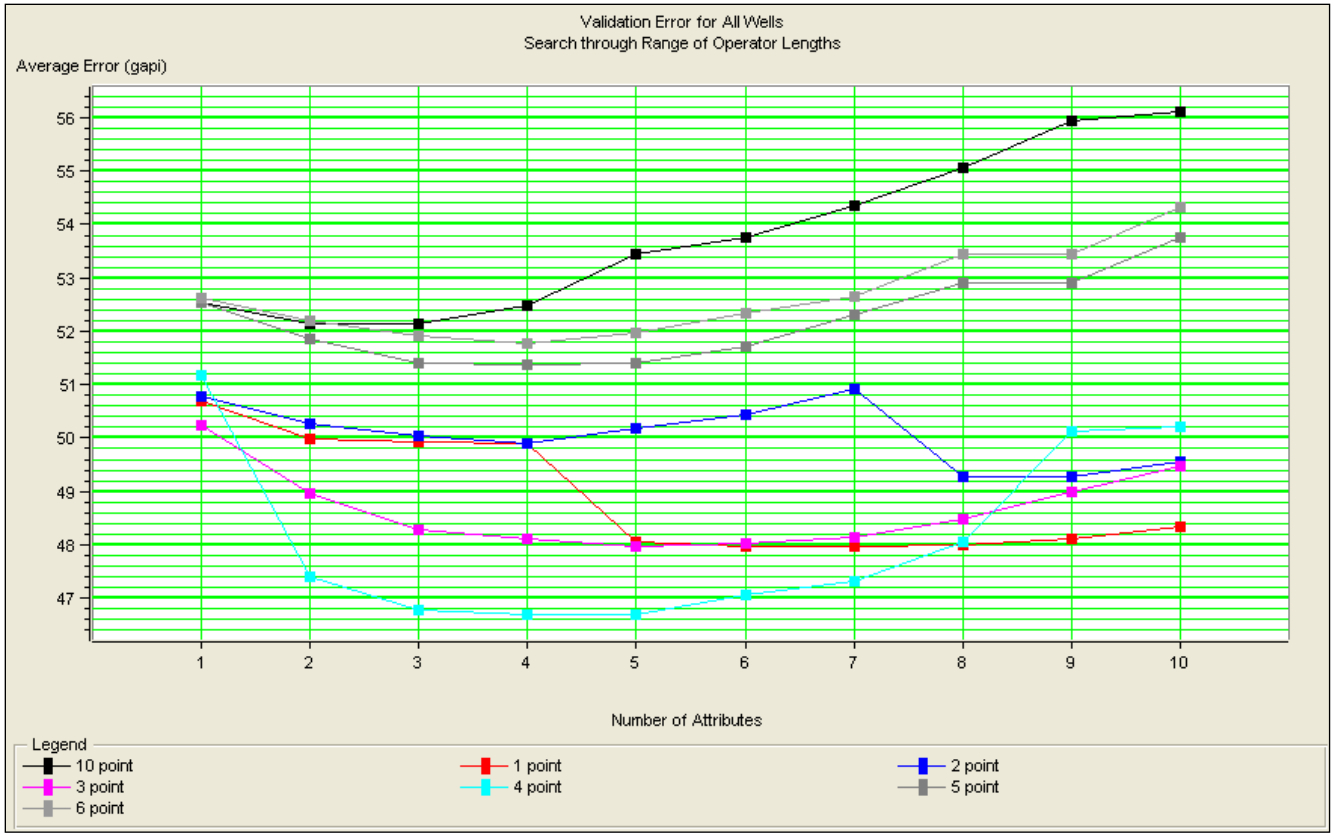

Figure 10. Validation error curve as the result of multi-attribute training process showing possible combinations of operator lengths and attributes. The best combination for the lowest average error is four point operators and five attributes (red circle).

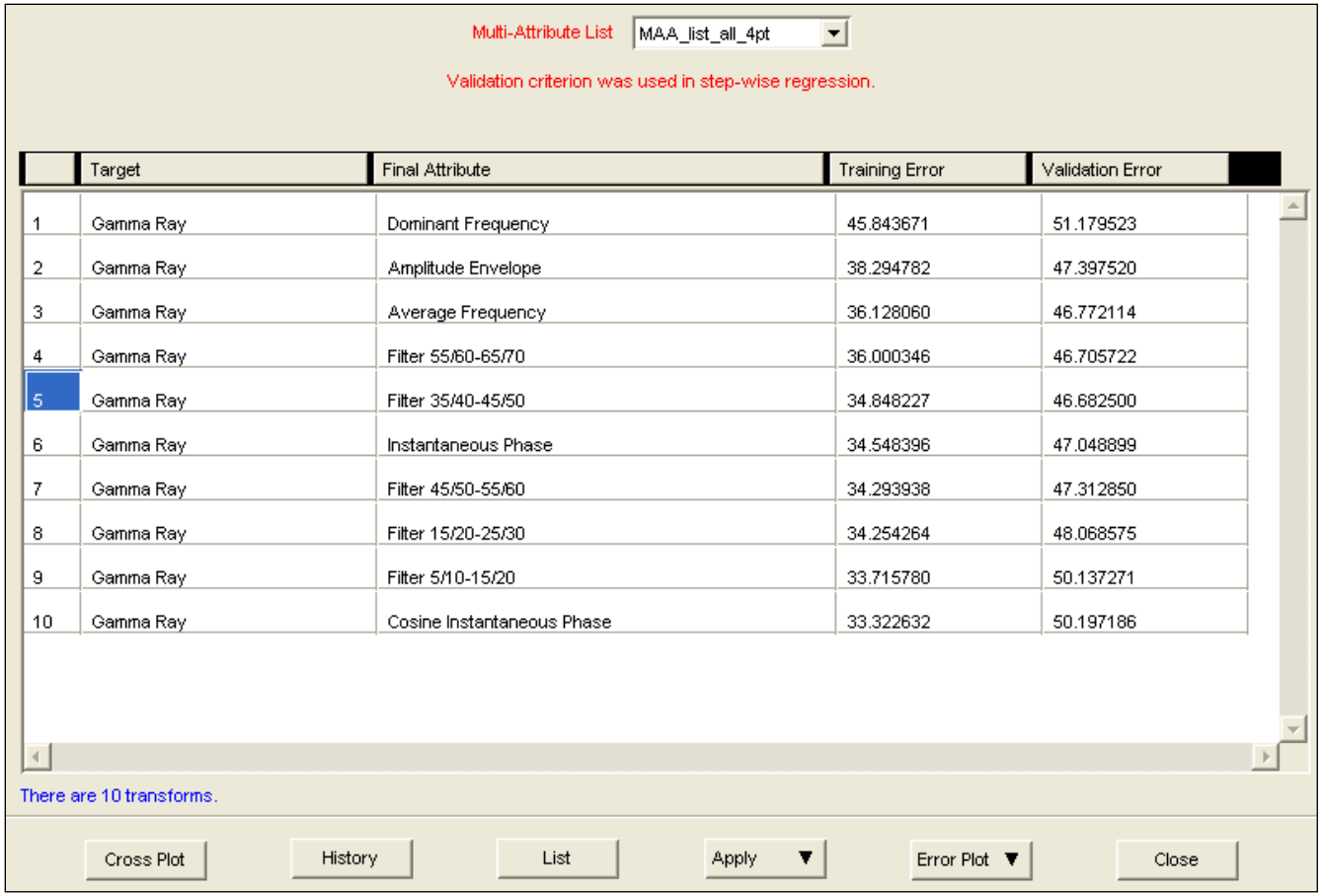

	Target	Final Attribute	Training Error	Validation Error
1	Gamma Ray	Dominant Frequency	45.843671	51.179523
2	Gamma Ray	Amplitude Envelope	38.294782	47.397520
3	Gamma Ray	Average Frequency	36.128060	46.772114
4	Gamma Ray	Filter 55/60-65/70	36.000346	46.705722
5	Gamma Ray	Filter 35/40-45/50	34.848227	46.682500
6	Gamma Ray	Instantaneous Phase	34.548396	47.048899
7	Gamma Ray	Filter 45/50-55/60	34.293938	47.312850
8	Gamma Ray	Filter 15/20-25/30	34.254264	48.068575
9	Gamma Ray	Filter 5/10-15/20	33.715780	50.137271
10	Gamma Ray	Cosine Instantaneous Phase	33.322632	50.197186

Figure 11. Types of seismic attribute and related training and validation errors for operator length of four points. The top five attributes (red rectangle) give the lowest average error of predicted gamma ray.

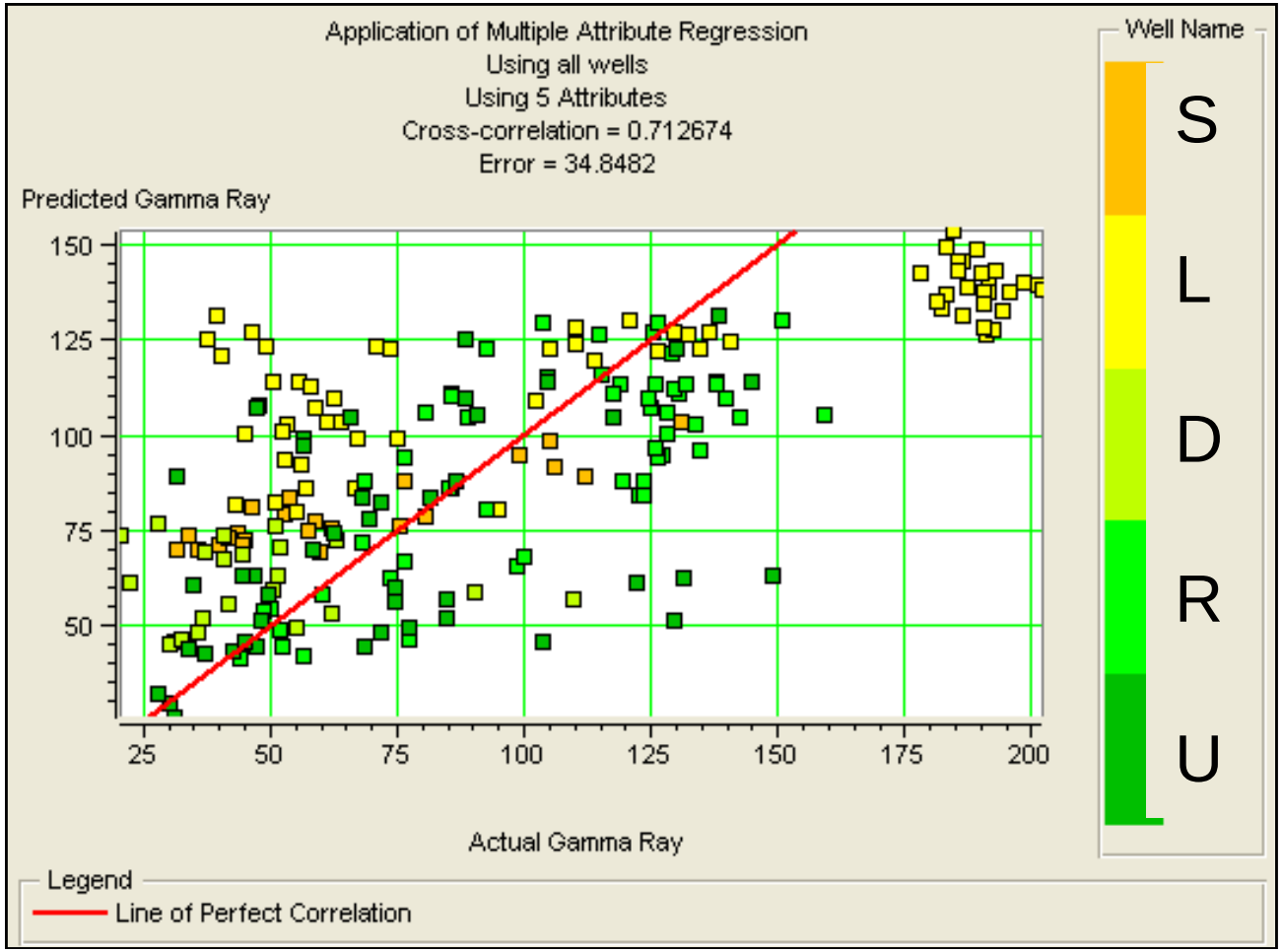

Figure 12. Cross-plot of predicted and actual gamma ray showing a correlation value of 0.71 with an error margin of 34.85 gAPI. Well L has the lowest cross-correlation value.

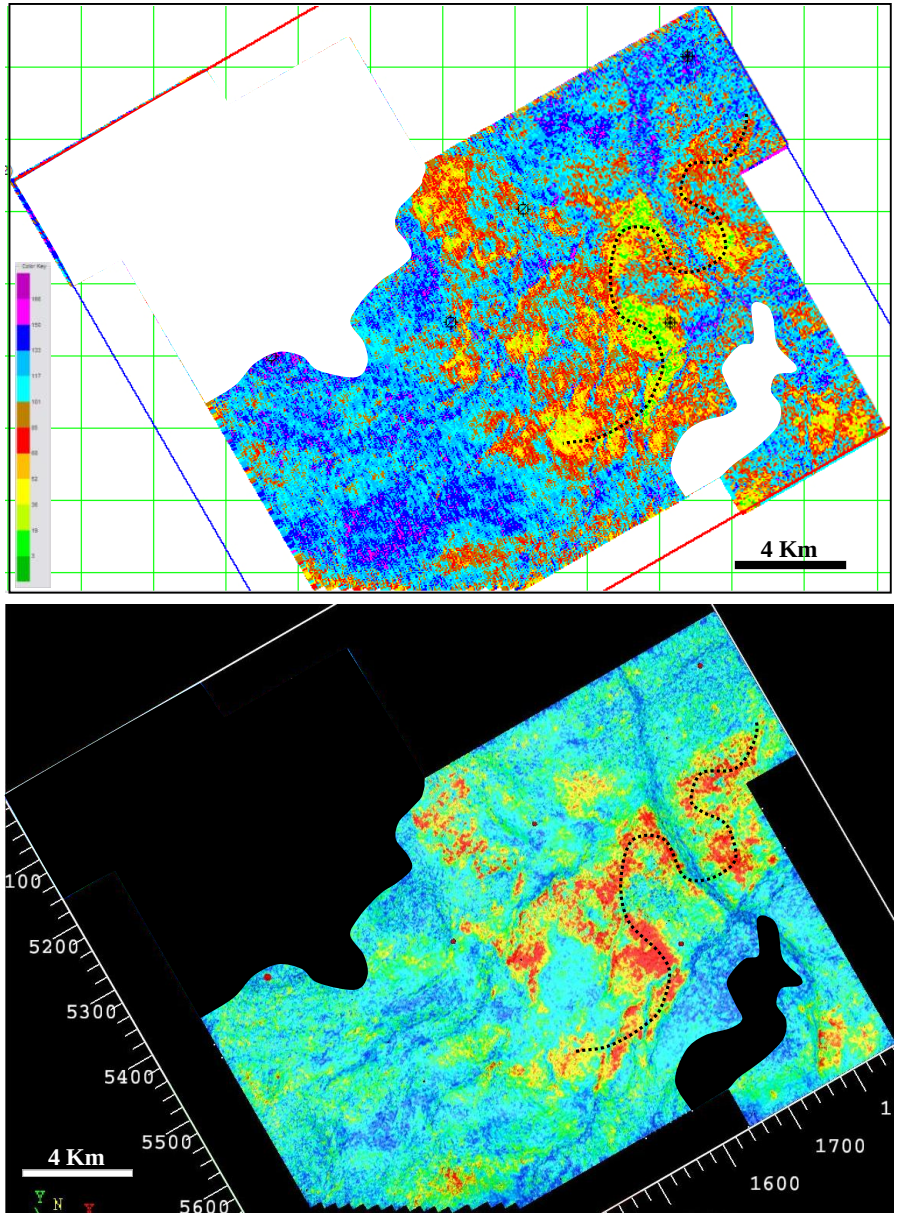

Figure 13. The peak amplitude trend at 25 Hz spectral decomposition map of the lower member (lower image) showing a consistent trend with the low gamma-ray values on predicted gamma-ray map (upper image). Both maps identify channel trend with direction of NE-SW in the eastern part of study area. The spectral decomposition was generated using the Maximum Entropy Method (MEM) algorithm.

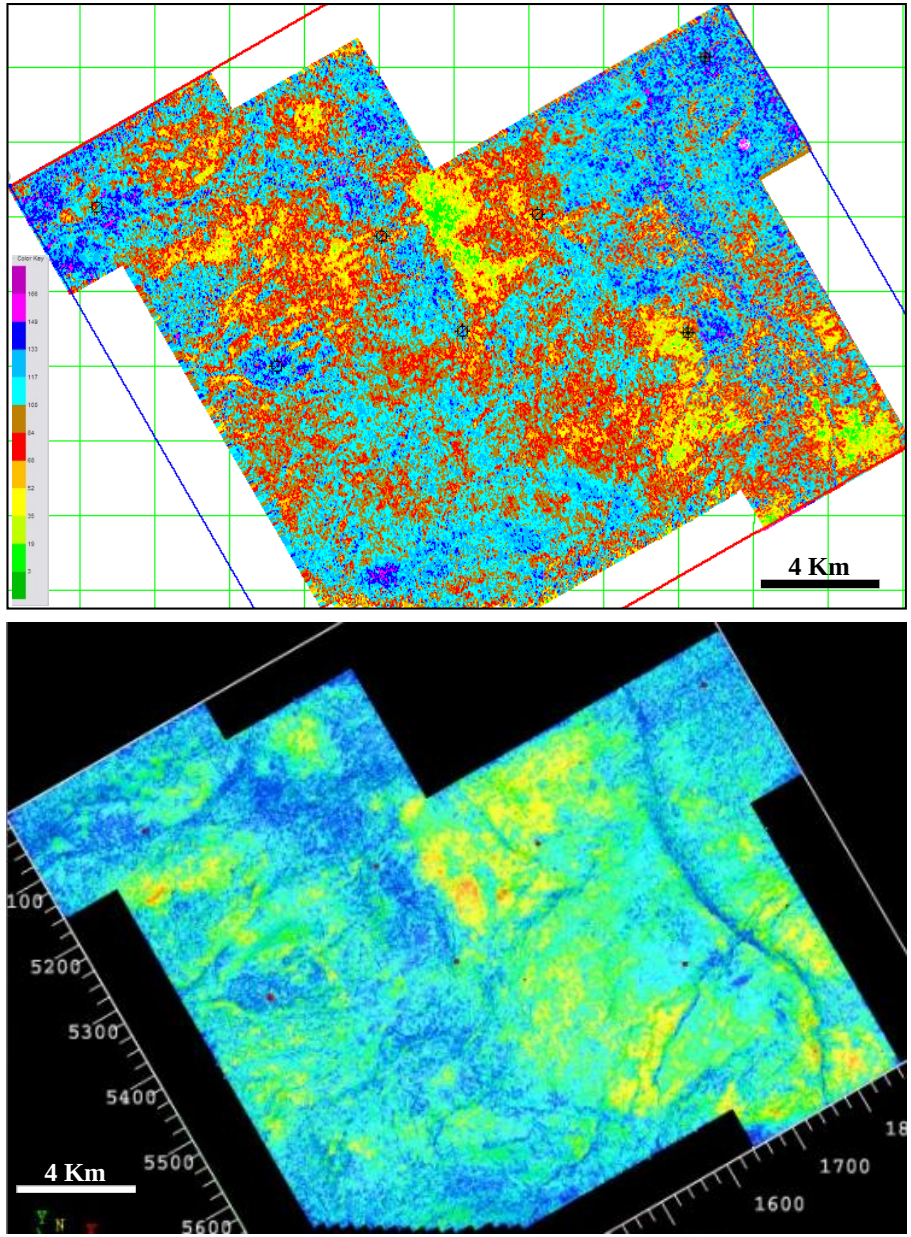

Figure 14. Spectral decomposition map of the upper member (UTAF) at 25 Hz (lower image) showing an approximate NW-SE trend with predicted gamma-ray map (upper image). The spectral decomposition was generated using the Maximum Entropy Method (MEM) algorithm with 20 ms analysis window. According to the maps, most exploration wells were drilled in the relatively poor sandstone area.

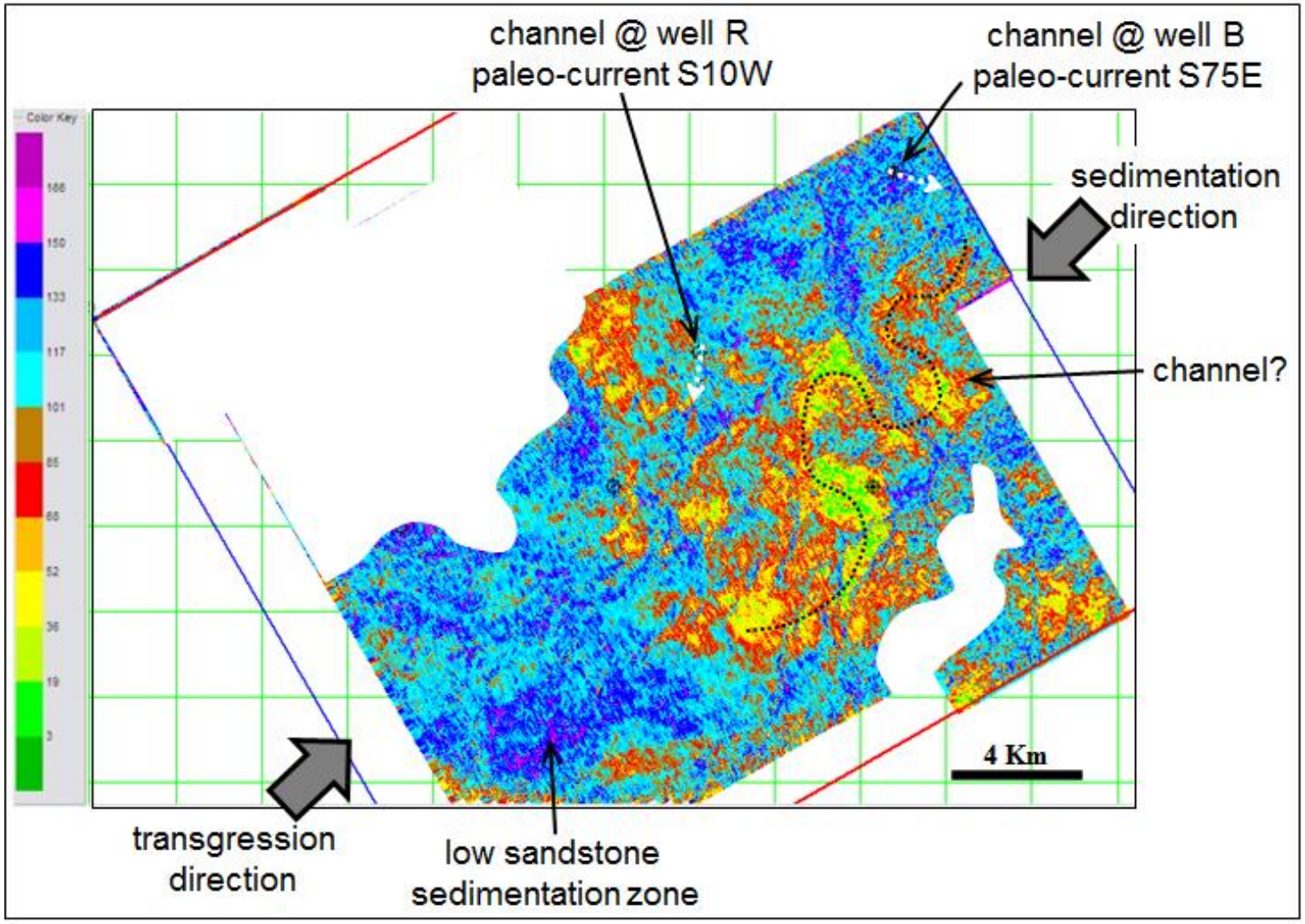

Figure 15. RMS map of predicted gamma ray for the lower member. Geological interpretation identifies a channel feature in the eastern part of the study area.

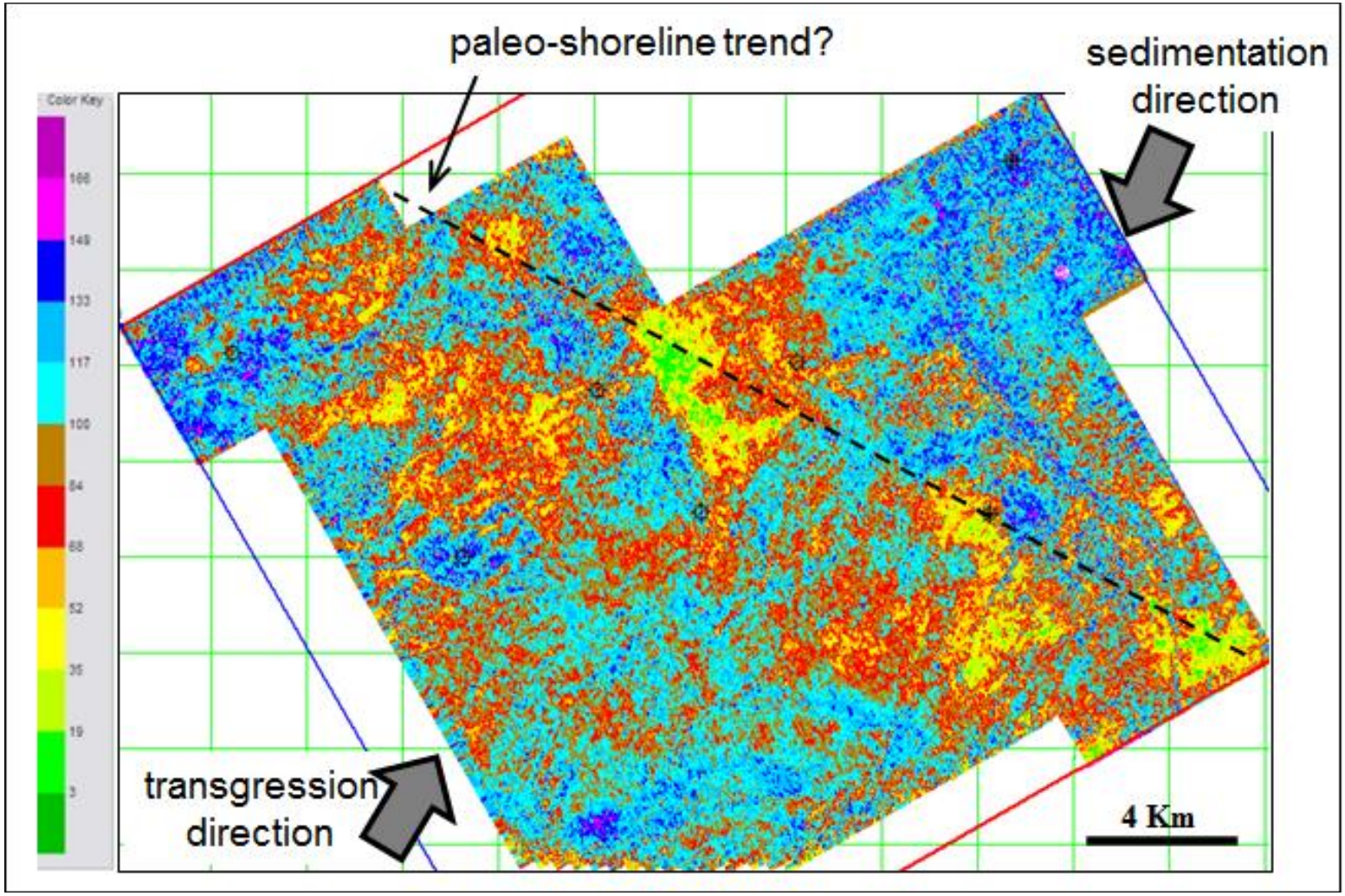

Figure 16. RMS map of predicted gamma ray for the upper member. Geological interpretation identifies a possible paleo-shoreline trend (approximately NW-SE) represented by the sandstone distribution.

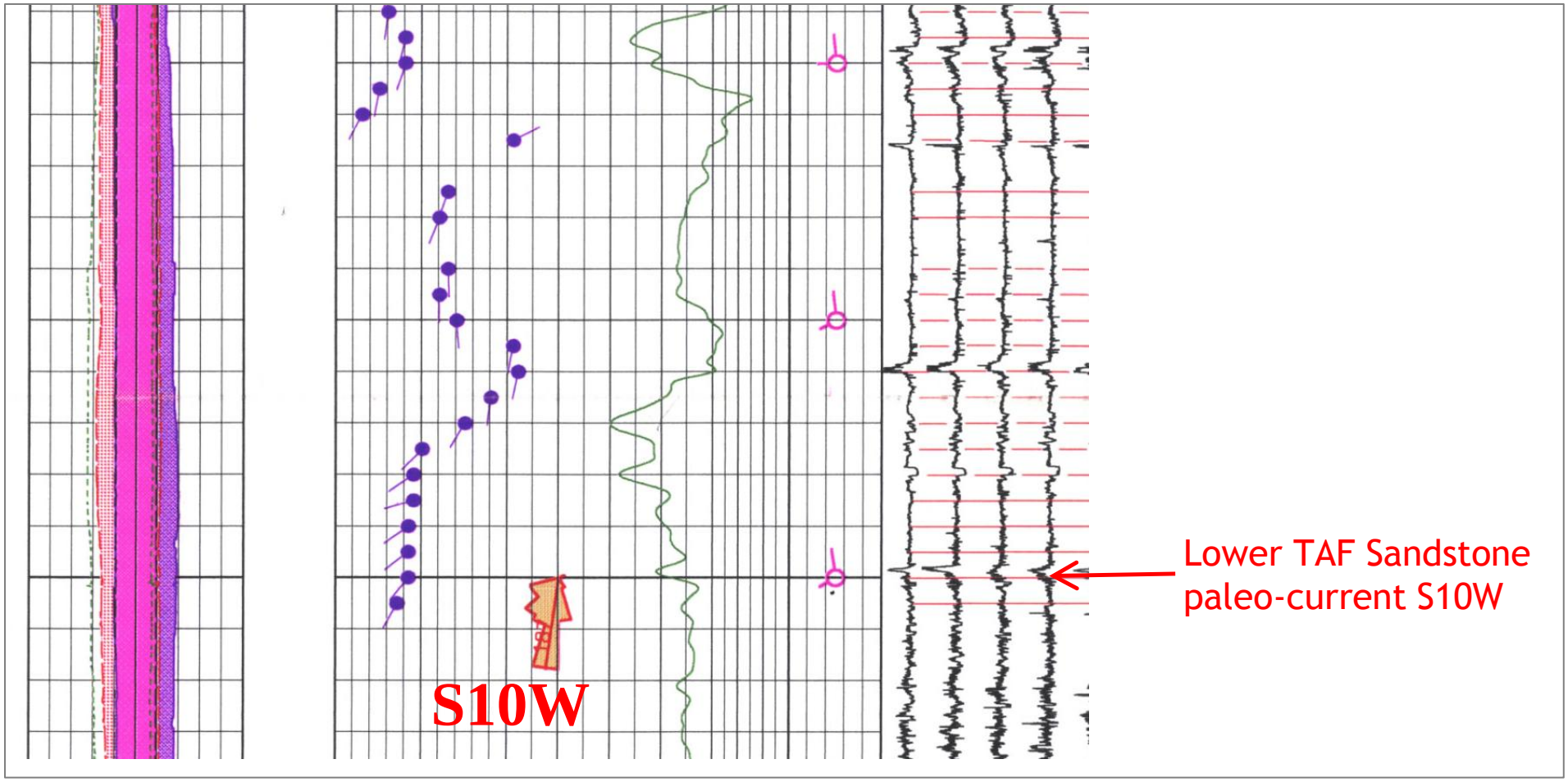

Figure 17. Dip log of well R showing a sandstone layer within the lower member (LTAF) with paleo-direction to the southwest (S10W).

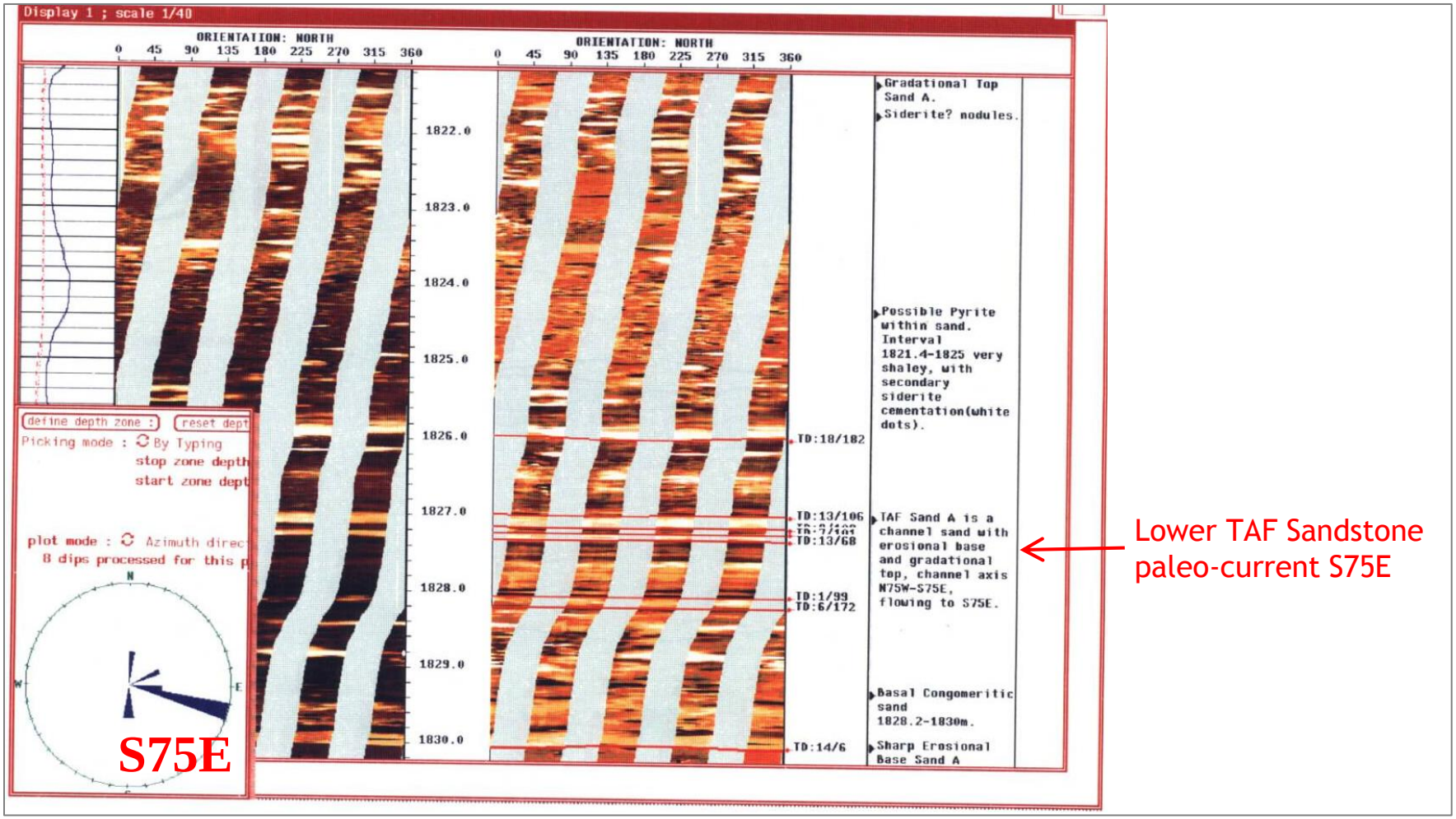

Figure 18. Image log (FMI - Formation Micro Imager) of well B showing a channel sand layer within the lower member (LTAF) with paleo-direction to the east-southeast (S75E).

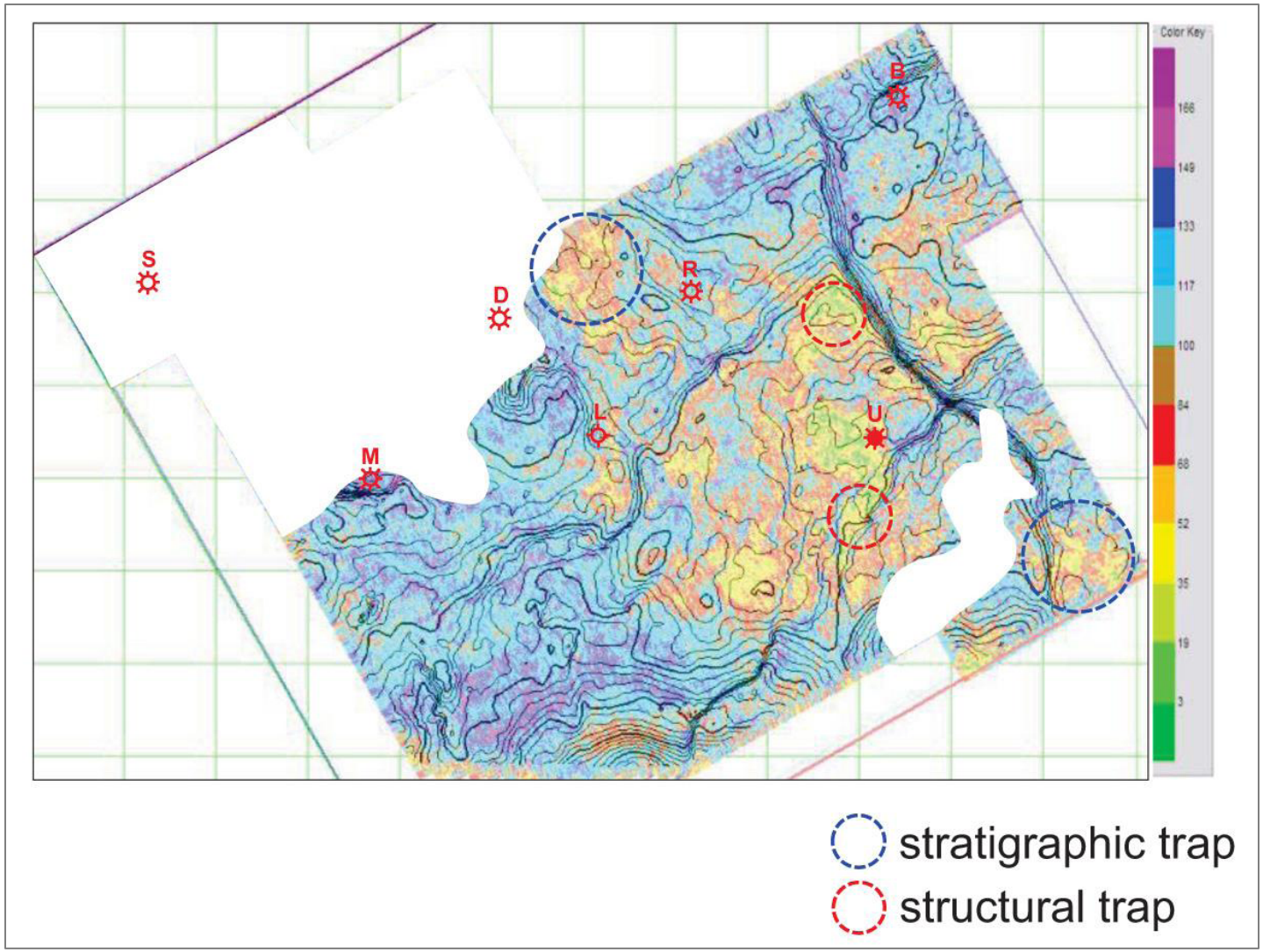

Figure 19. Depth structure and predicted GR map, LTAF, with potential traps.

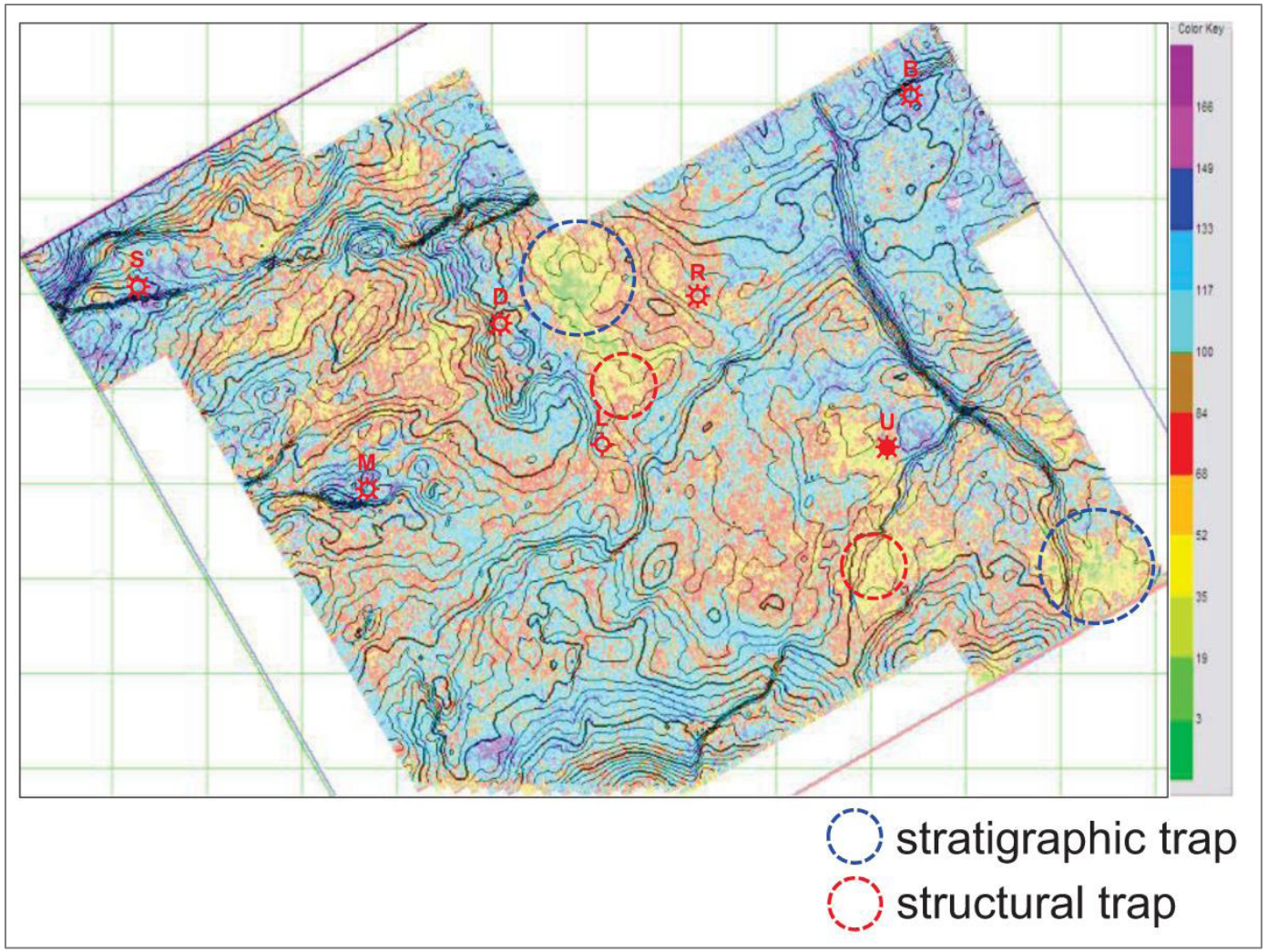

Figure 20. Depth structure and predicted GR map, UTAF, with potential traps.